Plant Physiol. (1995) 109: 963–972

Effects of Iron Limitation on Photosystem II Composition and Light Utilization in *Dunaliella tertiolecta*[1]

Ilya R. Vassiliev[2], Zbigniew Kolber, Kevin D. Wyman, David Mauzerall, Vipula K. Shukla, and Paul G. Falkowski*

Oceanographic and Atmospheric Sciences Division, Department of Applied Science, Brookhaven National Laboratory, Upton, New York 11973–5000 (I.R.V., Z.K., K.D.W., P.G.F.); Rockefeller University, New York, New York 10021 (D.M.); and Department of Biology, Washington University, St. Louis, Missouri 63130 (V.K.S.)

The effects of iron limitation on photosystem II (PSII) composition and photochemical energy conversion efficiency were studied in the unicellular chlorophyte alga *Dunaliella tertiolecta*. The quantum yield of photochemistry in PSII, inferred from changes in variable fluorescence normalized to the maximum fluorescence yield, was markedly lower in iron-limited cells and increased 3-fold within 20 h following the addition of iron. The decrease in the quantum yield of photochemistry was correlated with increased fluorescence emission from the antenna. In iron-limited cells, flash intensity saturation profiles of variable fluorescence closely followed a cumulative one-hit Poisson model, suggesting that PSII reaction centers are energetically isolated, whereas in iron-replete cells, the slope of the profile was steeper and the calculated probability of energy transfer between reaction centers increased to >0.6. Immunoassays revealed that in iron-limited cells the reaction center proteins, D1, CP43, and CP47, were markedly reduced relative to the peripheral light-harvesting Chl-protein complex of PSII, whereas the α subunit of cytochrome b_{559} was about 10-fold higher. Spectroscopic analysis established that the cytochrome b_{559} peptide did not contain an associated functional heme. We conclude that the photochemical conversion of absorbed excitation energy in iron-limited cells is limited by the number of photochemical traps per unit antenna.

Iron is the most abundant transition metal in the Earth's crust and is an essential element in the prosthetic groups of many biochemical constituents of the photosynthetic apparatus (Raven, 1990). In the open ocean, the major source of iron is aeolian dust derived from the continents (Duce and Tindale, 1991). Despite its abundance in crustal rocks, the concentration of iron in large areas of the world ocean is so low (subnanomolar) that the element can limit photosynthesis in natural phytoplankton (Martin, 1992). Iron limitation is easily detected by increases in F_o and marked decreases in variable fluorescence (Greene et al., 1992). These two phenomena reflect a loss of photochemical energy conversion efficiency in PSII (Greene et al., 1992). The limitation is rapidly reversed by the addition of exogenous soluble iron (Greene et al., 1992; Kolber et al., 1994). Here we examine the biophysical and biochemical basis of iron limitation in PSII in a model eukaryotic marine alga, *Dunaliella tertiolecta*.

D. tertiolecta is a strictly photoautotrophic, unicellular chlorophyte with a single cup-shaped chloroplast and a photosynthetic apparatus similar to that of higher plants (Berner et al., 1989). Previous studies with this alga established that iron limitation leads to a reduction in total cellular Chl with almost no change in the Chl *a/b* ratio (Greene et al., 1992). From measurements of variable fluorescence, we found that, whereas F_v/F_m values decreased as *D. tertiolecta* became iron limited, there was an increase in σ_{PSII}. Moreover, kinetics analysis of the decay of variable fluorescence revealed that the half-time for the oxidation of Q_A^- increased 2-fold, and quantitative analysis of western blots revealed that the reaction center protein D1 and Cyt *f* and subunit IV (the plastoquinone-docking protein) of the Cyt b_6/f complex were significantly reduced under iron-limited conditions. From analysis of ^{59}Fe autoradiographs of proteins isolated by SDS-PAGE and from western blot analyses, the recovery of maximum photochemical efficiency in PSII appeared to be correlated with the incorporation of Fe into Cyt b_{559} and a concomitant decrease in F_o (Greene et al., 1992). Similar effects were found in iron-limited cells of the cyanobacterium *Anacystis nidulans*, which had a high F_o level and extremely low variable fluorescence, indicating a decrease in the number of functional (i.e. charge separating) PSII reaction centers (Reithman and Sherman, 1988). Although these results suggest that iron availability affects the number of functional PSII reaction centers, it could also significantly alter the

[1] This research was supported by the U.S. Department of Energy under contract No. DE-AC02–76CH00016. V.K.S. was supported by a predoctoral fellowship from the Monsanto Co.

[2] Present address: Department of Biochemistry, University of Nebraska, Lincoln, NE 68588–0664.

* Corresponding author; e-mail falkowsk@bnlux1.bnl.gov; fax 1–516–282–3246.

Abbreviations: ASW, artificial seawater medium; $\Delta\phi_{sat}$, the maximum change in the quantum yield of fluorescence (= F_v/F_o); F_m, maximal Chl fluorescence yield, emitted when PSII centers are closed; F_o, minimal (constant) fluorescence yield, emitted when PSII centers are open following dark adaptation; F_v, variable fluorescence yield (= $F_m - F_o$); LHCII, peripheral light-harvesting Chl-protein complex of PSII; Q_A, primary quinone acceptor of PSII; Q_B, second electron accepting plastoquinone of PSII; σ_{PSII}, effective absorption cross-section of PSII; σ_o, the intrinsic absorption cross-section of PSII; *T*, reaction center of PSII trap density (traps per photosynthetic domain).

efficiency of energy transfer from the antenna to the reaction centers.

Iron deficiency can lead to a loss of functional PSII reaction centers, a decrease in excitation energy transfer from LHCII to the reaction centers, or both. Using low-temperature Chl fluorescence spectroscopy and variable fluorescence techniques, we studied the fate of absorbed energy in PSII in iron-limited *Dunaliella*. Parallel analyses of core proteins, using western blot and herbicide-binding techniques, suggest a 3- to 4-fold decrease in the number of PSII reaction centers relative to LHCII. Analysis of the changes in σ_{PSII} and the extent of energy transfer between PSII reaction centers suggests that the photochemical conversion of excitation energy is limited by the density of PSII reaction centers per unit effective antenna. By following the kinetics of the recovery from iron limitation in *Dunaliella*, we examined the relationship between reaction center density and the efficiencies of energy transfer and excitation trapping in PSII.

MATERIALS AND METHODS

Cell Growth Conditions

Stock cultures of *Dunaliella tertiolecta* Butcher (Woods Hole clone DUN) were grown in 1-L polycarbonate flasks in an ASW enriched with f/2 nutrients (Guillard and Ryther, 1962). Chelated iron, as $FeCl_3(6H_2O)$/EDTA, was added to a final concentration of 250 nM Fe. Cells were grown in 1-L polycarbonate flasks at 18°C with constant aeration and mixing, under continuous light (250 μmol quanta m^{-2} s^{-1}) provided by banks of cool-white fluorescent tubes. Iron-limited cells were harvested from early stationary-phase cultures (7×10^5 cells mL^{-1}) by centrifugation and transferred to iron-depleted (no added iron) ASW (Greene et al., 1992). The photochemical efficiency of PSII in whole cells was estimated from the relative variable fluorescence yield, F_v/F_m (see below). It usually took about 4 d for the cells to attain a low, steady-state value of F_v/F_m of about 0.20, compared with approximately 0.6 for iron-replete cells. The recovery from iron limitation was initiated by adding 250 nM (final concentration) $FeCl_3(6H_2O)$/EDTA. Following the iron addition, we measured cell numbers, cellular Chl concentration, and in vivo Chl fluorescence and prepared samples for low-temperature fluorescence spectroscopy at several times. Additionally, protein analyses and herbicide-binding studies were performed on iron-limited cells and iron-replete cells. Three independent sets of experiments were performed on the recovery from iron limitation; representative data are presented.

Cell Numbers and Chl Concentration

Cell numbers were determined with a hemacytometer. Chls *a* and *b* were measured in 90% acetone extracts using the equations of Jeffrey and Humphrey (1975).

Chl Fluorescence Induction

Fluorescence induction curves were measured on optically thin cell suspensions adapted to darkness for 5 min following the addition of 10 μM DCMU. The samples, containing between 0.6×10^6 and 1.0×10^6 cells mL^{-1} (approximately 0.2 μg Chl mL^{-1}) were placed in a 1-cm pathlength cuvette in an optically isolated chamber close to the end window of a Hamamatsu (Bridgewater, CT) R565 photomultiplier. Actinic illumination (3×10^{16} quanta cm^{-2} s^{-1}) from an Oriel (Stratford, CT) model 66011 xenon arc lamp was directed to the front of the cuvette by a fiber optic light guide and controlled by a Uniblitz (Vincent Associates, Rochester, NY) SD122B electronic shutter (full opening time, 1 ms). Broad-band blue light was isolated with a Corning (Corning, NY) 4–96 filter and passed through an IR and UV filter. A Corning 2–64 filter was used to isolate the fluorescence wavelengths. The amplified fluorescence signals were digitized with an ADC488/SA 12-bit A/D converter (IOtech Inc., Cleveland, OH).

Pump and Probe Fluorescence

Pump and probe fluorescence measurements were made using a custom-built pump and probe fluorometer described by Kolber et al. (1988). Actinic pump flashes had a 1.6-μs half-peak duration and a maximum flux of approximately 10^{16} quanta cm^{-2}. The energy of the probe flash was attenuated to 0.5% of the actinic flash and had a half-peak duration of 0.7 μs. Fluorescence from the probe flash was measured before (designated F_o) and 80 μs following (designated F) a pump flash of variable energy. Flash intensity saturation curves were numerically analyzed to estimate the effective absorption cross-section for PSII, the probability of energy transfer between PSII reaction centers, and T size. The change in the quantum yield of fluorescence ($\Delta\phi = [F - F_o]/F_o$) as a function of the photon exposure from the actinic flash was initially fit to a cumulative one-hit Poisson distribution,

$$\Delta\phi = \Delta\phi_{sat}[1 - \exp(-\sigma_{PSII}E)]$$

where $\Delta\phi_{sat}$ is the change in maximum fluorescence yield ($[F_m - F_o]/F_o$), σ_{PSII} is the effective absorption cross-section of PSII (Å^2 quanta^{-1} per trap), and E is flash energy (Ley and Mauzerall, 1982; Falkowski et al., 1986). The data from iron-limited cells could be fit with this simple expression, which implies no energy transfer between traps, or, to be more correct, equal probability of transfer between open and closed traps. For the remaining data, the curves were fit with the modified algorithm of Ley and Mauzerall (1986) using inverse methods. This model has the following parameters: *a*, the probability of escape from a closed trap to find an open reaction center; *b*, the probability of "escape" from an open trap; and T, the number of traps per domain. The result is a very weak function of T for values >4. The numerical solution revealed *b* to vary between 0 and 0.1. Thus, the relevant parameter, *a*, varied from near 0 in iron-limited cells to 0.6 in iron-replete cells.

Low-Temperature Fluorescence Spectroscopy

Iron-depleted and iron-replete cells were harvested by centrifugation, resuspended in 70% glycerol to a Chl ($a + b$) concentration of 5 μg mL^{-1} in 1.5-mm i.d. quartz tubes,

and flash frozen in liquid nitrogen under dim green light. Quantum corrected fluorescence excitation and emission spectra were measured at 77 K with an SLM/Aminco (Rochester, NY) 4800 spectrofluorometer using an internal standard and equipped with a low-temperature accessory. For precise quantitation, each sample was measured at eight different orientations of the tube, and the average spectrum was calculated. For excitation spectra, both the excitation and emission monochromator slits were set to 1 nm. For measurements of emission spectra, the excitation monochromator slit width was set to 4 nm at a wavelength of 435 nm and the emission monochromator slit width to 0.5 nm. Analytical deconvolution of the spectra was performed in the frequency domain, assuming a gaussian distribution of the excited states.

Protein Analysis

For isolation of thylakoid membranes, cells were harvested by centrifugation and washed in isolation medium consisting of 50 mM Tris-maleate buffer (pH 7.4) and 10 mM NaCl. Cells were disrupted on ice in 200 μL of isolation medium with 100 μM PMSF by three 30-s sonication cycles using a Kontes (Vineland, NJ) microprobe sonicator at maximum power. Samples were centrifuged at 14,000 rpm in an Eppendorf microfuge for 5 min to remove debris, and the green supernatant, containing thylakoids, was mixed with 2 mL of isolation medium. PMSF and $MgCl_2$ were added to the suspension to final concentrations of 100 μM and 50 mM, respectively, and the membranes were pelleted by centrifugation at 10,000*g* at 5°C for 15 min. The membrane pellet, containing mostly thylakoids, was washed twice in 50 mM Tris-maleate buffer (pH 7.4) containing 10 mM NaCl, 50 mM $MgCl_2$, and 100 μM PMSF and finally suspended in 100 μL of this buffer with 10% (v/v) glycerol. The membranes were flash frozen in liquid nitrogen and stored at −80°C.

For solubilization of membrane proteins, the thylakoids were centrifuged and resuspended in 100 μL of a buffer consisting of 100 mM Na_2CO_3, 4% SDS, and 100 μM PMSF, sonicated for 1 min using a Kontes microprobe sonicator on maximum power, and centrifuged at 14,000 rpm in an Eppendorf microfuge for 5 min. Small aliquots of the supernatant were used for determination of Chl concentration and total protein. Total protein was determined by the Pierce BCA assay using BSA as a standard. The remainder of the supernatant was diluted with an equal volume of 0.2 M DTT and 2 volumes of a solution containing 4% SDS, 15% glycerol, and 0.05% bromthymol blue and heated at 100°C for 2 min. Proteins were separated by SDS-PAGE using a Bio-Rad minigel system, with a 7% stacking and 15% resolving gel. Samples containing between 10 and 25 μg of protein were loaded into each lane and run at constant voltage (145 V) for 1.5 to 2 h at room temperature. Following electrophoresis, proteins were visualized with Coomassie blue or by silver staining.

Electrophoretic transfer of proteins to nitrocellulose was performed using a Phast System (Pharmacia). Proteins were separated on 20% homogeneous gels, transferred to nitrocellulose, challenged with polyclonal antibodies raised against the proteins of interest, and visualized with an alkaline phosphatase reporter (Bennett et al., 1984). Three to five replicate western blots were analyzed for each protein. Gels and western blots were quantified with a Molecular Dynamics (Sunnyvale, CA) 300B laser densitometer.

Radiolabeled Herbicide-Binding Assay

Herbicide-binding sites were quantified following the basic procedure described by Vermaas et al. (1990). Cells were washed twice with ASW and adjusted to give a final Chl (a + b) concentration of 20 μg mL^{-1}. The cells were incubated for 20 min in darkness and mixed in 1.5-mL Eppendorf tubes with varying concentrations of ^{14}[C]-atrazine (Sigma; specific activity, 57 μCi mg^{-1}). To correct for nonspecific atrazine binding, half of the treatments contained 20 μM nonlabeled DCMU. After a 20-min incubation with the herbicides under dim green light, the suspensions were centrifuged and 800-μL aliquots of supernatant were mixed with scintillation cocktail and counted in an LKB (Pharmacia) scintillation counter. Three replicates were taken for each concentration of radiolabeled herbicide, both in the absence and in the presence of DCMU. The herbicide-binding dependency was calculated by subtracting the amount of free ^{14}[C]atrazine in samples containing DCMU from that in samples without DCMU and fitted to a hyperbolic equation:

$$C_{bound} = K\,C_{max}/(K + C_{free}),$$

where C_{bound} and C_{free} are concentrations of specifically bound and free herbicide, K is the binding constant, and C_{max} is the concentration of binding sites determined from nonlinear regression analysis.

Spectroscopic Estimation of Cyt b_{559}

Thylakoids were isolated as described and solubilized in Triton X-100 (Boeringer Mannheim) to a final concentration of detergent:Chl of 25:1 (w/w). Insoluble material was removed by centrifugation at 15,000*g* for 10 min, and the supernatant was diluted in 100 mM sorbitol, 50 mM Hepes (pH 7.5), 5 mM $MgCl_2$, and 10 mM NaCl to a final Chl concentration of 100 μM (+Fe samples) or 620 μM (−Fe samples). Measurement of Cyts was performed on an SLM/Aminco DW2000 spectrophotometer in the dual-beam mode, with a reference wavelength at 540 nm and a half-bandwidth of 0.1 nm. Potassium ferricyanide was added to a final concentration of 200 μM, and the sample was equilibrated at room temperature in the dark for 15 min. Five scans between 500 and 600 nm were averaged and taken as the oxidized spectrum. For determination of Cyt f, hydroquinone was added to a final concentration of 1 mM and the absorption measured as described above. For detection of Cyt b_6 and b_{559}, a few grains of dithionite were added and the spectra were measured as described. Cyt b_{559} heme was quantified from the dithionite minus hydroquinone difference spectrum as described by Whitmarsh and Ort (1984) using an extinction coefficient of 17.5 mM^{-1} cm^{-1} (Cramer et al., 1986).

RESULTS

Physiological Characteristics of Iron-Limited *Dunaliella*

The addition of iron to iron-limited cells led to a 2-fold increase in cellular Chl concentration within 24 h. The change in Chl/cell preceded a 2-fold increase in the specific growth rate calculated from the time-dependent changes in cell numbers (Fig. 1A). The change in total cellular Chl was not accompanied by any statistically significant change in the ratio of Chl *a/b*.

F_v, normalized to F_m (i.e. F_v/F_m), values were as low as 0.17 to 0.23 in iron-limited cells, compared with 0.6 in iron-replete cells (Fig. 1B). The addition of iron induced a large and rapid (<10 h) decrease in both F_o and F_m (normalized to Chl *a*). The change in F_o preceded the increase in variable fluorescence, and F_v/F_m reached values of 0.52 to 0.58 within 20 h (Fig. 1B). Thus, the depressed F_v/F_m ratios in iron-limited cells are primarily a consequence of high F_o values relative to F_m, suggesting that a large fraction of the absorbed excitation energy is emitted from the pigment bed rather than photochemically coupled to PSII.

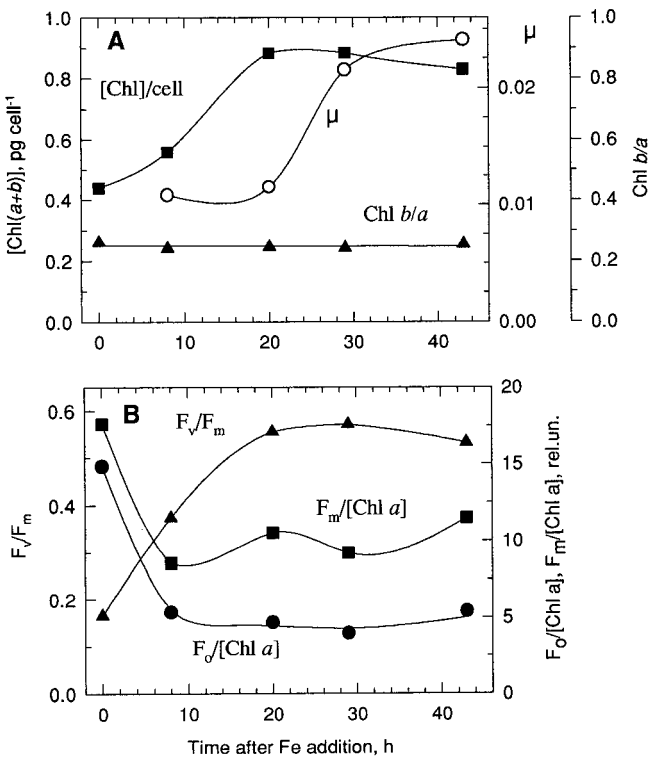

Figure 1. A, Changes in cellular Chl, specific growth rate, and the Chl *b/a* ratio following the addition of 250 nM chelated $FeCl_3(6H_2O)$ to an iron-limited culture of *D. tertiolecta*. The specific growth rate was calculated as $\mu = 1/t \ln(N_t/N_o)$, where t is time, N_o is initial cell density, and N_t is cell density at time t. B, Changes in F_o and F_m and the normalized variable fluorescence yields (F_v/F_m) during the course of recovery from iron limitation measured by fluorescence induction in the presence of 20 μM DCMU. The intensities of F_o and F_m were normalized to Chl and therefore represent the relative quantum yields of fluorescence.

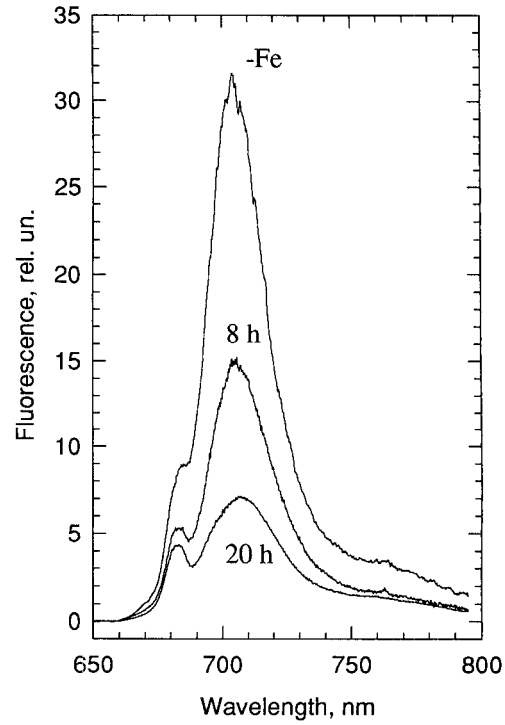

Figure 2. Low-temperature (77 K) fluorescence emission spectra of intact cells of *D. tertiolecta* measured at different times following addition of iron to the growth medium. The spectra were recorded at constant Chl values and normalized with an internal standard; thus the relative units (rel. un.) represent changes in the yields.

77 K Fluorescence Spectra

Low-temperature fluorescence excitation/emission spectra were obtained with and without the addition of glycerol. Whereas the fluorescence emission profiles were not qualitatively affected by the cryoprotectant (in fact, glycerol is a major storage product in *Dunaliella*; Ben-Amotz and Avron, 1973), the apparent fluorescence yields obtained in the absence of glycerol were significantly lower as a consequence of light scattering. Thus, we opted to use glycerol to improve the signal-to-noise ratio in the excitation and emission spectra, thereby facilitating improved resolution of the emission bands in the decomposition analyses.

When excited at 435 nm, the low-temperature fluorescence emission spectra displayed multiple emission bands, with a broad maximum at approximately 710 nm, a shoulder at 682 nm, and a broad, flat, far-red component without a distinct peak (Fig. 2). The excitation signature for the 710-nm emission band is virtually identical with that found for the 682-nm band in both iron-depleted and -replete cells (Fig. 3). Low-temperature fluorescence emission at 685 and 695 nm is generally attributed to the PSII core antennae pigment proteins, CP43 and CP47, respectively (Krause and Weis, 1991), whereas emission at 720 to 740 nm is ascribed to PSI (Mimuro, 1993). However, the origin of emission in the 695- to 715-nm spectral region in green algae and higher plants is unclear, with some evidence for the contribution of either PSII peripheral antenna (Zuccelli

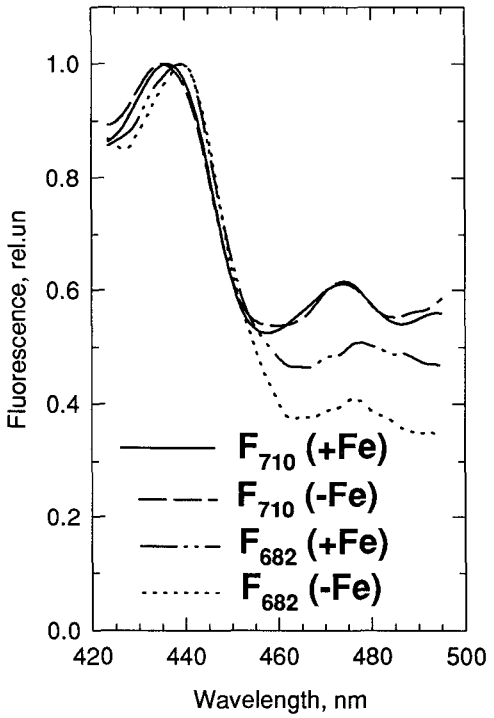

Figure 3. Representative 77 K fluorescence excitation spectra of iron-replete (+Fe) and iron-depleted (−Fe) cells of *D. tertiolecta* measured at emission wavelengths of 710 and 682 nm. rel. un., Relative units.

et al., 1992; Jennings et al., 1993) or PSI components (Karapetyan et al., 1980; Kramer et al., 1985; Mimuro, 1993). In *D. tertiolecta*, the low-temperature emission at 710 nm is excited by both 440- and 475-nm light; the latter corresponds to absorption bands of Chl *b* and carotenoids in LHCII (Sukenik et al., 1987).

Within 20 h following the addition of iron, the fluorescence yield from the 710-nm band decreased by about 5-fold, whereas the 682-nm component was relatively unaffected. The fluorescence yields and spectral profiles of the emission bands at 77 K measured 20 h following the addition of iron were indistinguishable from control cells that had been grown in iron-replete media. The time course and magnitude of the decrease in fluorescence yield of the 710-nm band at low temperature closely corresponded to the increase in F_v/F_m at room temperature. These results and the correspondence between the decrease in F_o/Chl and the emission at 77 K during recovery from iron limitation suggest that the 705- to 715-nm emission band originates from a light-harvesting antenna serving PSII.

Analytical decomposition of the fluorescence emission spectra of iron-depleted and iron-replete cells is shown in Figure 4. The analysis revealed the presence of six components in the spectrum of iron-replete cells with peaks at 674, 682, 694, 704, 714, and 751 nm. There were two major differences between the spectra of iron-depleted and iron-replete cells. First, iron-depleted cells lacked the 694-nm component. Second, when the spectra were normalized to the 751-nm band, the 702- to 704- and 713- to 714-nm components appeared to be the most affected by recovery from iron limitation. The increase in the yields of these components at 77 K in iron-limited cells corresponds with the increase in the F_o levels at room temperature. These results suggest that the changes in both low-temperature and room-temperature fluorescence yields originate from one or more of the four light-harvesting Chl protein complexes that make up LHCII in *D. tertiolecta* (Sukenik et al., 1987, 1988).

Effective Absorption Cross-Section of PSII

σ_{PSII} is a function of the optical absorption cross-section of the antenna serving PSII reaction centers and the efficiency of the excitation transfer from the antenna to the reaction centers. Energy transfer is manifested in the fluorescence saturation curve as rising more steeply than pre-

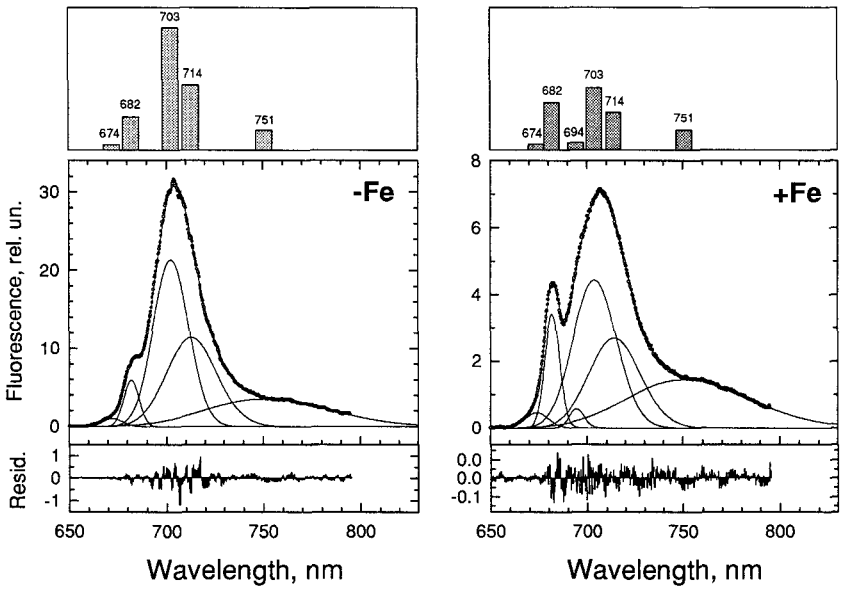

Figure 4. Decomposition analysis of 77 K fluorescence emission spectra of iron-replete (+Fe) and iron-depleted (−Fe) cells of *D. tertiolecta* fitted to gaussian components. Histograms on the top show the relative values of the amplitudes of the individual components normalized to the emission at 751 nm; the bottom of the histograms shows the calculated residuals (Resid.) for the best fit of the data to the individual components. rel. un., Relative units.

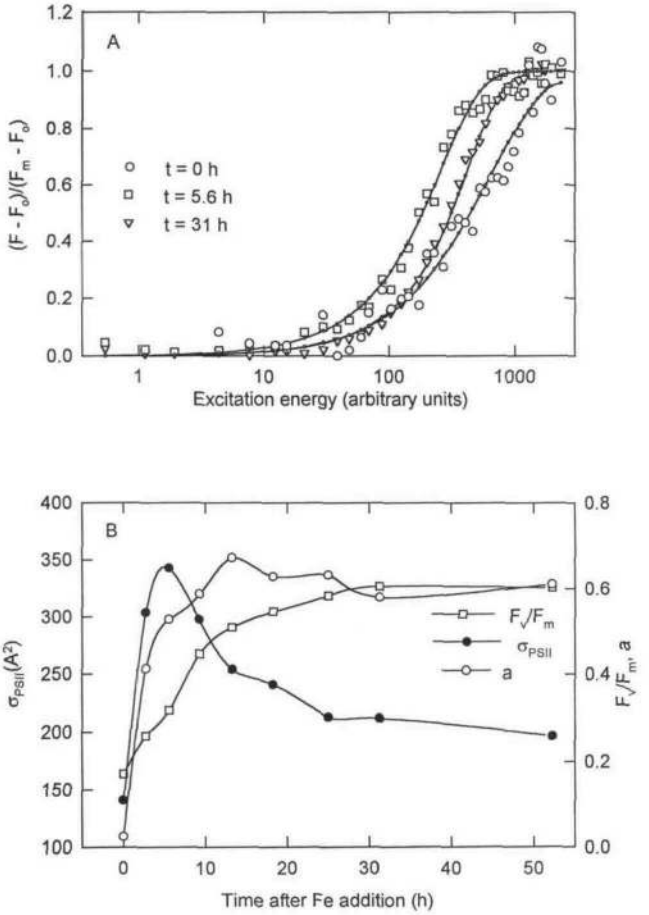

Figure 5. A, Representative flash intensity saturation profiles of variable fluorescence for severely iron-limited cells of *D. tertiolecta* (t = 0 h) and for cells at 5.6 and 30 h following the addition of iron. The data were derived with a pump and probe fluorescence technique as described by Falkowski et al. (1986). The curves are the fit of the experimental data to the energy transfer model described by Ley and Manzerall (1986). B, Time course of the changes in σ_{PSII}, F_v/F_m, and the probability of escape from a closed reaction center, a, following the addition of iron.

dicted by a cumulative one-hit Poisson function (Ley and Mauzerall, 1986; Mauzerall and Greenbaum, 1989). The effective absorption cross-section increases if more antenna molecules are connected to a domain but decreases as T increases.

A relatively complex pattern of σ_{PSII} emerged during recovery from iron limitation (Fig. 5). Under extreme iron limitation, σ_{PSII} was initially minimal and then increased rapidly to a maximum within 5 h following the addition of iron. It subsequently declined asymptotically, reaching a steady-state level after about 30 h. The flash intensity saturation profiles differed significantly between iron-limited cells and those recovering from iron limitation; curves for the former closely followed a cumulative one-hit Poisson function, whereas the latter displayed characteristics indicative of a high probability of energy transfer between PSII reaction centers (Fig. 5A). Under extreme iron limitation, the probability of energy transfer approached zero. The reduction in effective cross-section and energy transfer in iron-depleted cells coincided with decreased efficiency of excitation trapping, which is indicated by extremely low F_v/F_m values (Fig. 5B), and with high levels of radiative losses in the pigment bed, as indicated by high F_m/Chl (Fig. 1).

Within 5 h following the addition of iron, σ_{PSII} increased markedly and the probability of energy transfer increased from about 0 to about 0.6. In the subsequent recovery period, σ_{PSII} decreased with a half-time of approximately 15 h and was paralleled by decreases in F_v/F_m. In contrast, a and F_m/Chl a remained relatively constant. These data suggest that during this period the observed changes in the σ_{PSII} were controlled primarily by the changes in the efficiency of excitation trapping within the antenna. The quantum yield of photochemistry in PSII (= F_v/F_m) increased from 0.15 to 0.30 during the first 5 h following the addition of iron. It reached 0.62 in the second phase. The 2-fold increase in Φ_{PSII} in the second phase of recovery was accompanied by about a 1.5-fold decrease in σ_{PSII}. These results can be explained by the rapid reconnection of uncoupled antenna groups to photochemically functional domains, causing an apparent doubling of the size of the unit. This is then followed by the addition of newly activated or synthesized reaction centers, which reduces the size of the unit by approximately half.

PSII Composition

The decrease of energy-trapping efficiency in PSII reaction centers upon iron limitation might be caused by structural degradation of components of the PSII complex and/or by impairment of primary photochemical reactions within PSII due to a loss of electron transport carriers. When equal concentrations of proteins were loaded on gels, with the exception of an increased stained band at 47 kD, the protein-banding patterns of solubilized thylakoid membranes for iron-replete and iron-depleted samples were remarkably similar (Fig. 6, A and B).

Quantitation of the western blots (Fig. 6C) revealed significant differences in the abundance of PSII polypeptides

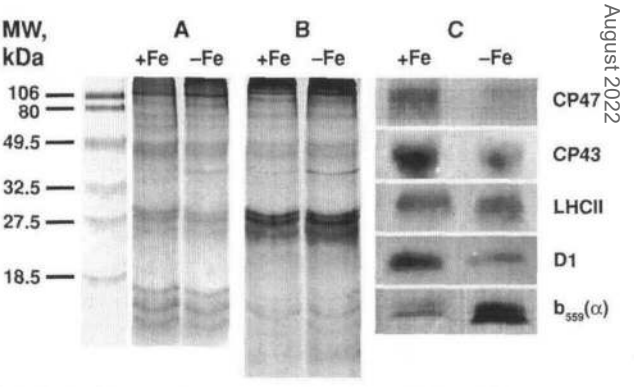

Figure 6. SDS-PAGE patterns of solubilized thylakoid membrane proteins of iron-replete (+Fe) and iron-depleted (−Fe) cells of *D. tertiolecta* stained with Coomassie blue (A) or silver (B). Western blots of SDS-PAGE-separated PSII polypeptides, loaded on an equivalent protein basis and probed with polyclonal antibodies (C). MW represents molecular mass.

in iron-depleted and control samples relative to total membrane protein (Table I). The content of D1, CP43, and CP47 in iron-depleted thylakoids was about 65% of corresponding protein in iron-replete thylakoids, whereas the relative abundance of the α subunit of Cyt b_{559} was about 1 order of magnitude higher in iron-depleted than in iron-replete samples.

Quantitation of RCII

The area above the fluorescence induction curve in the presence of DCMU is proportional to the fraction of photochemically reduced Q_A (Malkin and Kok, 1966). Based on this analysis, the ratio of reducible Q_A in iron-replete/iron-deficient cells was 3.9/1; i.e. there are approximately 4-fold more PSII reaction centers per unit effective antenna in iron-replete cells. Analysis of the herbicide-binding assays suggests an atrazine/Chl ratio of 1.5 and 5.8 μmol/mol for iron-depleted and iron-replete membranes, respectively (Fig. 7). Thus, the three independent estimates of reaction centers of PSII, namely the immunoassay of D1, the area over the fluorescence induction curve in the presence of DCMU, and the herbicide-binding assay, correspond to a loss of D1, ranging from 65 to 75% of the iron-replete membranes, relative to LHCII or total proteins. We consider these results to be internally consistent; the differences are not statistically significant given the precision of the methods.

Quantification of Cyt b_{559}

The calculated molar ratio of Chl (a + b) to Cyt b_{559} heme in iron-replete thylakoid membranes from *D. tertiolecta* averaged 2760. Even though we used Chl concentrations 6-fold higher to assay for Cyt b_{559} heme, the Cyt was barely detectable in the iron-deficient thylakoids.

DISCUSSION

Iron is an important cofactor in Chl biosynthesis, and chlorosis is a well known and universal indication of iron limitation (Guikema and Sherman, 1983; Nishio et al., 1985; Greene et al., 1992). In iron-limited *D. tertiolecta*, cellular Chl declined by 50%; however, both the Chl *a/b* ratio and the protein-specific abundance of LHCII were virtually identical with that in iron-replete thylakoid membranes. It is, therefore, highly unlikely that the 3-fold decrease in photochemical energy conversion efficiency is a consequence of biochemical alterations in the peripheral antenna complexes serving PSII. The decrease in variable fluorescence is due primarily to an increase in F_o, which, based on the analysis of fluorescence lifetimes, appears to be, in turn, a consequence of a decrease in radical pair formation in PSII reaction centers (Falkowski et al., 1994). Is this decrease due to a large fraction of photochemically incompetent reaction centers, as occurs under heat stress or photoinhibitory conditions in algae, or to an uncoupling of energy transfer from the antenna to the reaction centers?

Table I. *Relative abundance of PSII polypeptides in thylakoids from iron-depleted and iron-replete D. teriolecta cells estimated by laser densitometry of western blots (see Fig. 6C)*

The average amounts of each protein and their SDs were calculated on the basis of "sum over background" for three replicate blots using Image Quant software (Molecular Dynamics). The results are the means ± SD.

Protein	−Fe	+Fe
D1	25.0 ± 8.3	73.3 ± 1.5
Cyt b_{559} (α)	42.4 ± 8.7	4.2 ± 0.6
CP47	11.4 ± 2.9	31.9 ± 0.9
CP43	38.8 ± 1.7	106.4 ± 7.3
LHCII	62.3 ± 9.2	54.9 ± 18.6

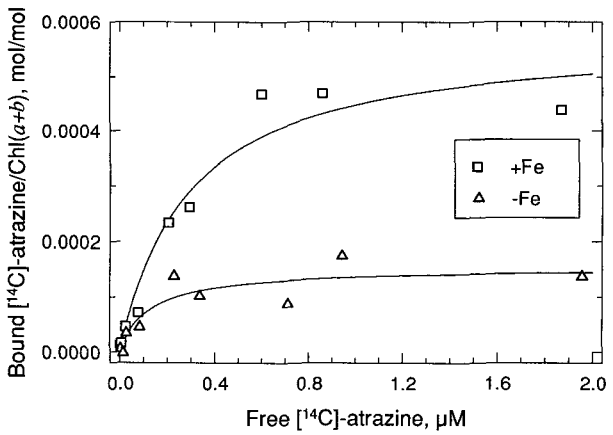

Figure 7. Herbicide-binding dependencies of iron-replete (□) and iron-depleted (△) *D. tertiolecta* cells. Lines are hyperbolic fits of experimental data. The binding constants are 0.13 and 0.29, and atrazine/Chl (mol/mol) ratios are 0.00015 and 0.00058 for iron-depleted and iron-replete cells, respectively.

Composition of PSII Components

The effects of iron limitation on PSII excitation-trapping efficiency are reflected in the low-temperature fluorescence emission spectra; the quantum yield of fluorescence under iron-limited conditions is up to 6-fold higher than in iron-replete cells. Upon addition of iron, fluorescence at 682 nm, which is ascribed to CP43, increases markedly relative to that at 710 nm. Unlike in cyanobacteria or isolated PSII particles from higher plants (Krause and Weis, 1991), there is no distinct emission band at 695 nm corresponding to CP47 in *D. tertiolecta*, and yet deconvolution analysis of iron-replete cells reveals a component at 694 nm that cannot be resolved in iron-deficient cells.

Quantitative analysis of western blots clearly reveals that, when compared on an equal LHCII basis, the PSII reaction center proteins, D1, CP43, and CP47, are markedly reduced in the iron-limited thylakoids. Moreover, analyses of functional PSII reaction centers, based on the area over the induction curve in DCMU-poisoned cells and herbicide binding, suggest that in iron-limited cells the decrease in reaction centers of PSII per unit LHCII is proportional to the loss of core antenna complexes.

In contrast to these changes, the α subunit of Cyt b_{559} accumulated to a much higher level than that found in iron-replete cells. The optically based oxidized minus re-

duced difference spectra from these samples established, however, that the large pool of apoprotein in the iron-limited cells lacked a functional heme. Although the function of Cyt b_{559} remains obscure, Cyt b_{559} deletion mutants have no photochemical activity in PSII (Pakrashi et al., 1989). The addition of iron to iron-deficient mutants restores photochemical activity in PSII much more rapidly than the synthesis of the protein components in PSII would suggest (Greene et al., 1992). Moreover, a time-course analysis of autoradiographs of SDS-PAGE proteins from iron-limited cells incubated with ^{59}Fe reveals that one of the first proteins to become labeled corresponds to Cyt b_{559}. The synthesis of heme is controlled in the cytoplasm, and post-translational assembly of Cyts in plastids normally requires the coordinated synthesis of the peptides with the heme (Howe and Merchant, 1994). Our results suggest that, in part, the rapid restoration of photochemical activity is a consequence of heme biosynthesis, allowing previously synthesized Cyt b_{559} apoproteins to rapidly assemble into electrochemically functional components of PSII reaction centers. Although this hypothesis clearly requires data before it can be verified (e.g. we do not have information about the β subunit), the data imply that in iron-limited *D. tertiolecta* the syntheses of heme and Cyt b_{559} apoproteins are uncoupled.

Iron also plays an important role in PSII by coordinating D1 and D2 and in directing conformational changes essential to efficient electron transfer between Q_A and Q_B (Vermaas et al., 1994). This nonheme iron is not electrophoretically stable and, hence, is not visible in ^{59}Fe-labeled autoradiographs of SDS-PAGE proteins. If, however, iron-limited cells lacked the nonheme iron and synthesized D1, it might be expected that the reaction center protein would accumulate in the membranes in excess. This is not the case, and we propose that the loss of functional reaction centers is not a direct consequence of the loss of nonheme iron, although iron limitation may limit the assembly of D1-D2 heterodimers. The possibility of some unassembled D1 emerges from the atrazine-binding assays, which suggest a 2-fold lower binding constant for the herbicide in iron-depleted membranes. Based on site-directed mutation of D1 in *Synechocystis* sp. PCC 6803, Vermaas et al. (1994) suggested that the nonheme iron affects both herbicide binding and Q_A reduction in the D1-D2 heterodimer. The rate constants for electron transfer between Q_A and Q_B are markedly lower in iron-deficient cells (Greene et al., 1992), possibly as a consequence of a lack of the nonheme iron in some reaction centers. Numerous attempts to analyze for the nonheme iron by electron paramagnetic resonance spectroscopy in *D. tertiolecta* thylakoid membranes were unsuccessful.

PSI also has iron-containing components that serve as cofactors of photosynthetic electron transport (for review, see Golbeck, 1992); in fact, more iron is associated with PSI than PSII (Raven, 1988). In cyanobacteria, iron limitation leads to a marked decrease in the content of F_X, F_A, and F_B iron-sulfur clusters, with an accompanying loss of electron transport capacity and growth (Sandmann and Malkin, 1973). The effects of iron limitation on the biophysical properties of PSI have not been extensively studied in eukaryotic algae, but the lack of iron can lead to the induction of alternate electron transport components in PSI, such as flavodoxin (LaRoche et al., 1993). Although we did not specifically examine PSI energetics in this study, we note that the low-temperature fluorescence emission centered at 751 nm, which originates from PSI antenna, was about 3-fold higher in iron-limited cells and decreased more rapidly compared with the major PSII emission band at 710 nm (Fig. 4). The elevated fluorescence yield at 751 nm in iron-limited cells suggests that the limitation reduces excitation-trapping efficiency in PSI, and the rapid decrease in the fluorescence yield following the addition of iron suggests that the repair process is capable of quickly assimilating exogenous iron and incorporating the element into the key prosthetic groups in PSI, even while PSII photochemistry is impaired. In iron-replete *D. tertiolecta*, the ratio of PSII to PSI is close to unity (Falkowski et al., 1981; Sukenik et al., 1987). Although the apparent favoring of PSI repair over PSII following iron addition to the iron-deficient cells may lead to a transient imbalance in the excitation of the two photosystems, it may provide energy from PSI cyclic electron flow that may be used for biosynthetic processes.

Energy Transfer and Trapping

The kinetics of recovery from iron limitation reveals two distinctively different phases, suggesting that two phenomena are affected by the limitation. Initially, in iron-depleted cells, the high rate of radiative de-excitation losses (reflected by increased F_m/Chl *a*; Fig. 1) is accompanied by a small value of *a*, the probability of excitation bypassing closed reaction centers. Under such conditions, a significant fraction (about 60%) of the LHCII complexes does not transfer excitation energy directly to PSII reaction centers (Fig. 5B). This uncoupling is further manifested in a large increase in the fluorescence yield at 710 nm at 77 K. Our calculations suggest that under severe iron limitation the average *T* approaches the limit value of unity. In effect, severe iron limitation leads to an energetic isolation of PSII reaction centers.

The steep, transient increase in σ_{PSII} during the first 5 h of recovery from iron limitation is accompanied by an increase in F_v/F_m (Fig. 5B). Coinciding with these changes is the increase in the probability in the energy transfer between PSII reaction centers, from values close to 0 to approximately 0.6. There is no evidence from the flash intensity saturation profiles of multiple cross-sections for PSII (e.g. PSII heterogeneity); such a phenomenon would be manifested as flattening of the saturation profile at high excitation energies. The initial recovery from iron limitation is accompanied by increased efficiency of excitation trapping without large increases in cellular Chl (Figs. 1A and 5B), suggesting an increase in the coupling between extant antenna and nascent PSII reaction centers. This inference is supported by the time course of incorporation of ^{59}Fe into Cyt b_{559} (Greene et al., 1992), indicating that synthesis and/or assembly of PSII reaction centers occurs within a largely preexisting pigment bed.

As the recovery from iron limitation progresses, the density of functional reaction centers per LHCII unit increases, leading to a parallel increase in the efficiency of excitation trapping as indicated by decreased F_v/F_m. The changes in σ_{PSII} during this phase are controlled solely by the amount of LHCII serving PSII reaction centers through the energy transfer mechanisms. As the density of reaction centers increases, fewer antenna molecules serve more reaction centers, leading to a decrease in σ_{PSII}. In iron-replete cells, with the optimal ratio of functional reaction center of PSII/LHCII, the efficiency of the excitation trapping reaches a maximum and is optimized by energy transfer between reaction centers.

CONCLUSIONS

Our results suggest that in severely iron-limited cells the relative composition of PSII proteins becomes unbalanced, and the energy-trapping characteristics of PSII exemplify the biophysical construct of isolated photosynthetic units. Both the low trap density and the low efficiency of energy transfer from LHCII to functional reaction center of PSII results in a vanishingly low probability of photochemical trapping of absorbed energy in PSII. As cells recover from iron limitation, reaction center of PSII density rapidly increases and the nascent traps compete with each other for excitation energy within the antenna. This process leads to a connected unit structure and results in both a reduction in the effective absorption cross-section of each PSII and an increase in the quantum yield of photochemistry. The initial stage of recovery appears to be related to the incorporation of heme into Cyt b_{559}; the specific role of this electron carrier in PSII photochemistry remains enigmatic.

ACKNOWLEDGMENTS

The authors thank R.M. Greene for participation in experiments on absorption cross-section measurements. We thank William Cramer, Jean-Marc Ducruet, Julian Eaton-Rye, Ondrej Prasil, and Julie LaRoche for discussions and suggestions and W. Mangel for use of the SLM 4800 spectrofluorometer. The D1 antibody, raised against a synthetic peptide of a conserved region of the protein, was provided by Autar Mattoo and Marvin Edelman; the CP43 antibody was provided by John Mullet; the CP47 antibody was provided by Natan Nelson; the antibody to LHCII was raised against the complex from peas and was given by John Bennett. William Cramer kindly provided the antibody to the α subunit of Cyt b_{559}.

Received February 22, 1995; accepted July 14, 1995.

LITERATURE CITED

Ben-Amotz A, Avron M (1973) The role of glycerol in osmotic regulation of the halophylic alga *Dunaliella parva*. Plant Physiol **51:** 875–878

Bennett J, Jenkins GI, Hartley MR (1984) Differential regulation of the accumulation of the light-harvesting chlorophyll a/b complex and ribulose bisphosphate carboxylase/oxygenase in greening pea leaves. J Cell Biochem **25:** 1–13

Berner T, Dubinsky Z, Wyman K, Falkowski PG (1989) Photoadaptation and the "package" effect in *Dunaliella tertiolecta* (Chlorophyceae). J Phycol **25:** 70–78

Cramer W, Theg SM, Widger WR (1986) On the structure and function of cytochrome b_{559}. Photosynth Res **10:** 393–403

Duce RA, Tindale NW (1991) Atmospheric transport of iron and its deposition in the ocean. Limnol Oceanogr **36:** 1715–1726

Falkowski PG, Kolber Z, Mauzerall D (1994) A comment on the call to throw away your fluorescence induction apparatus. Biophys J **66:** 923–925

Falkowski PG, Owens TG, Ley AC, Mauzerall DC (1981) Effects of growth irradiance levels on the ratio of reaction centers in two species of marine phytoplankton. Plant Physiol **68:** 969–973

Falkowski PG, Wyman K, Ley AC, Mauzerall D (1986) Relationship of steady state photosynthesis to fluorescence in eucaryotic algae. Biochim Biophys Acta **849:** 183–192

Golbeck JH (1992) Structure and function of photosystem I. Annu Rev Plant Physiol Plant Mol Biol **43:** 293–324

Greene RM, Geider RJ, Kolber Z, Falkowski PG (1992) Iron-induced changes in light harvesting and photochemical energy conversion processes in eucaryotic marine algae. Plant Physiol **100:** 565–575

Guikema JA, Sherman LA (1983) Organization and function of chlorophyll in membranes of cyanobacteria during iron starvation. Plant Physiol **73:** 250–256

Guillard RRL, Ryther JH (1962) Studies of marine planktonic diatoms. I. *Cyclotella nana* (Hustedt) and *Detonula confervacea* (Cleve) Gran. Can J Microbiol **8:** 229–239

Howe G, Merchant S (1994) The biosynthesis of bacterial and plastidic c-type cytochromes. Photosynth Res **40:** 147–165

Jeffrey SW, Humphrey GW (1975) New spectrophotometric equations for determining chlorophylls a, b, c_1, and c_2 in higher plants, algae and natural phytoplankton. Biochem Physiol Pflanz **167:** 191–194

Jennings RC, Bassi R, Garlashi FM, Dainese P, Zucchelli G (1993) Distribution of the chlorophyll a spectral forms in the chlorophyll protein complexes of photosystem II antenna. Biochemistry **32:** 3202–3210

Karapetyan NV, Rakhimberdieva MG, Bukhov NG, Gyurjan I (1980) Characterization of photosystems of *Chlamydomonas reinhardtii* mutants differing in their fluorescence yield. Photosynthetica **14:** 48–54

Kolber Z, Zehr J, Falkowski PG (1988) Effects of growth irradiance and nitrogen limitation on photosynthetic energy conversion in photosystem II. Plant Physiol **88:** 72–79

Kolber ZS, Barber RT, Coale KH, Fitzwater SE, Greene RM, Johnson KS, Lindley S, Falkowski PG (1994) Iron limitation of phytoplankton photosynthesis in the Equatorial Pacific Ocean. Nature **371:** 145–149

Kramer HJM, Westerhuis WHJ, Amez J (1985) Low temperature spectroscopy of intact algae. Phyiol Veg **23:** 535–543

Krause GH, Weis E (1991) Chlorophyll fluorescence and photosynthesis: the basics. Annu Rev Plant Physiol Plant Mol Biol **42:** 313–349

LaRoche J, Geider RJ, Graziano LM, Murray H, Lewis K (1993) Induction of specific proteins in eucaryotic algae grown under iron-, phosphorus-, or nitrogen-deficient conditions. J Phycol **29:** 767–777

Ley A, Mauzerall D (1986) The extent of energy transfer among photosystem II reaction centers in *Chlorella*. Biochim Biophys Acta **850:** 234–248

Ley AC, Mauzerall D (1982) Absolute absorption cross sections for photosystem II and the minimum quantum requirement for photosynthesis in *Chlorella vulgaris*. Biochim Biophys Acta **680:** 95–106

Malkin S, Kok B (1966) Fluorescence induction studies in isolated chloroplasts. I. Number of components involved in the reaction and quantum yields. Biochim Biophys Acta **126:** 413–432

Martin JH (1992) Iron as a limiting factor in oceanic productivity. *In* P Falkowski, A Woodhead, eds, Primary Productivity and Biogeochemmical Cycles in the Sea. Plenum Press, New York, pp 123–137

Mauzerall D, Greenbaum NL (1989) The absolute size of a photosynthetic unit. Biochim Biophys Acta **974:** 119–140

Mimuro M (1993) Identification of the terminal energy donor to the reaction center in the pigment system of green plants by

time-resolved fluorescence spectroscopy at −196°C. Plant Cell Physiol **34:** 321–327

Nishio JN, Abadia J, Terry N (1985) Chlorophyll-proteins and electron transport during iron nutrition-mediated chloroplast development. Plant Physiol **78:** 296–299

Pakrashi HB, Diner BA, Williams JGK, Arntzen CJ (1989) Deletion mutagenesis of the cytochrome b_{559} protein inactivates the reaction center of photosystem II. Plant Cell **1:** 591–597

Raven JA (1988) The iron and molybdenum use efficiencies of plant growth with different energy, carbon and nitrogen sources. New Phytol **109:** 279–287

Raven JA (1990) Predictions of Mn and Fe use efficiencies of phototrophic growth as a function of light availability for growth and of C assimilation pathways. New Phytol **116:** 1–18

Reithman HC, Sherman LA (1988) Purification and characterization of an iron stress-induced chlorophyll-protein from the cyanobacteriun *Anacystis nidulans* R2. Biochim Biophys Acta **935:** 141–151

Sandmann G, Malkin R (1973) Iron-sulfur centers and activities of the photosynthetic electron transport chain in iron-deficient cultures of the blue-green alga *Aphanocapsa.* Plant Physiol **73:** 724–728

Sukenik A, Bennett J, Falkowski P (1988) Changes in the abundance of individual apoproteins of light-harvesting chlorophyll *a/b*-protein complexes of photosystem I and II with growth irradiance in the marine chlorophyte *Dunaliella tertiolecta.* Biochim Biophys Acta **932:** 206–215

Sukenik A, Wyman KD, Bennett J, Falkowski PG (1987) A novel mechanism for regulating the excitation of photosystem II in a green alga. Nature **327:** 704–707

Vermaas W, Charite J, Shen G (1990) Glu-69 of the D2 protein in photosystem II is a potential ligand to Mn involved in photosynthetic oxygen evolution. Biochemistry **29:** 5325–5332

Vermaas W, Vass I, Eggers B, Styring S (1994) Mutation of a putative ligand to the non-heme iron in photosystem II: implications for Q_A reactivity, electron transfer, and herbicide binding. Biochim Biophys Acta **1184:** 263–272

Whitmarsh J, Ort DR (1984) Stoichiometries of electron transport complexes in spinach chloroplasts. Arch Biochem Biphys **231:** 378–389

Zuccelli G, Jennings RC, Garlashi FM (1992) Independent fluorescence emission of the chlorophyll spectral forms in higher plant photosystem II. Biochim Biophys Acta **1099:** 163–169